Proceedings of the 29th Annual International
Conference of the IEEE EMBS
Cité Internationale, Lyon, France
August 23-26, 2007.

Characterization of Breast Tumors with NIR Methods using Optical Indices

Burak Alacam, Birsen Yazici
Dept. of Electrical, Computer, and Systems Engineering,
Rensselaer Polytechnic Institute,
Troy, NY, 12180

Britton Chance, Shoko Nioka
Dept. of Biochemistry and Biophysics,
University of Pennsylvania,
Philadelphia, PA, 19104

Abstract— **This work describes the characterization efficiency of optical properties of breast tumors based on the features obtained using *in vivo* near-infrared (NIR) spectroscopy measurements. Three features, relative blood concentration, oxygen saturation and the size of the tumor, are used to diagnose benign and malignant tumors. The performance of the proposed set of features are evaluated by various classifiers using data acquired from 44 patients with malignant tumors, and 72 patients with benign tumors. The area under the receiver operating characteristics (ROC) curve of the scaled nearest mean classifier (NMSC) using the three features yields a value of 0.91 with a significance level of 0.05. Our results suggest that the features, relative blood concentration, and oxygen saturation can differentiate breast tumors with a relatively high precision.**

I. Introduction

American cancer society (ACS) estimates that a total of approximately 200,000 new cases of invasive breast cancer occur in women in the United States every year [1]. Currently, there are over 2 million women living in the US who have been diagnosed with and treated for breast cancer. A total of 40,410 women and 470 men are predicted to die from breast cancer in the US during the year 2007 as per ACS estimates [1]. Breast cancer continues to be the leading cancer site among American women. *Early* detection is critical for effective treatment of breast cancer. Patients with tumors 1 cm or less in size have a greater than 90 percent long-term survival [2].

In recent years, there has been considerable interest in near-infrared (NIR) optical spectroscopy and tomography techniques since they provide contrast information that is specific to oxyhemoglobin, deoxyhemoglobin, and water which can potentially be used for *early* detection and diagnosis of breast cancer [3]–[8].

Correct interpretation of the optical indices (i.e. deoxyhemoglobin, oxyhemoglobin, blood volume, water content, scattering, and absorption) obtained by optical spectroscopic/tomographic techniques is also important as well as acquiring them. Several research groups demonstrated that the contrast in optical indices can provide information that allows for better characterization of breast cancer [3]–[5]. In [3], Pogue et al. presented a way to measure and obtain hemoglobin concentration, oxygen saturation, water fraction, scattering power, and scattering amplitude. These indices were then investigated for the differences between healthy and diseased breast tissues. In [4], Grosenick et al. reported on the optical indices, scattering and absorption coefficients, hemoglobin concentration, and blood oxygen saturation obtained using optical measurements. Their results showed that these optical indices can be used to distinguish carcinomas from healthy breast tissues. Recently, Khayat et al. [5] presented characterization results of optical indices, oxyhemoglobin, deoxyhemoglobin, blood volume, lipid and water content, scattering and absorption coefficients, using optical imaging. The results showed the ability of optical imaging to characterize different types of breast lesions.

In this work, we evaluated the characterization efficiency of optical properties of breast tumors using *in vivo* data obtained by near-infrared (NIR) spectroscopy. Our evaluation criteria is based on statistical classification techniques. Three features, namely, relative blood concentration, ΔBV, oxygen saturation, $\Delta Deoxy$, and the size of the tumor, S, were used to characterize benign and malignant tumors. The performance of the proposed set of features were evaluated using various classifiers on 44 patients with malignant tumors, and 72 patients with benign tumors. The area under the receiver operating characteristics (ROC) curve of the scaled nearest mean classifier (NMSC) using the three features yields a value of 0.91 with a significance level of 0.05.

The rest of the paper is organized as follows: In Section II, we present the NIR apparatus, and data protocol, followed by feature extraction and tumor classification. In Section III, we present statistical analysis of clinical data. Section IV summarizes our results.

II. Methods

A. Apparatus

In this study, a continuous wave (CW) near infrared spectrometer (NIRS) is used [9]. The apparatus includes a probe (Fig. 2). In the center of the probe there is a 3-wavelength light emitting diode (LED). The probe consisted of one multi-wavelength LED as a light source and 8 silicon diodes as detectors. The detectors surround the LED with a 4 cm radius. The light intensity from the detectors was adjusted to be approximately 1 volt and calibrated with a phantom with known absorption and scattering coefficients.

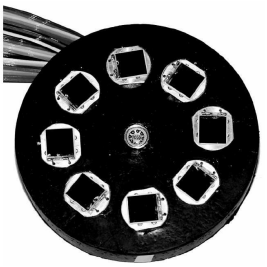

Fig. 1. The NIR probe with a multi-wavelength LED and 8 silicon diodes as detectors.

B. Patients and Protocol

This study includes two centers, namely, the Abramson Family Cancer Research Institute, Department of Radiology of the Hospital of University of Pennsylvania (HUP), and the Department of Gynecology of Leipzig University (DGLU). HUP provided 24 patients with malignant and 64 patients benign tumors. DGLU provided 20 patients with malignant and 6 benign tumors.

The measurements are taken on the breast with tumor. Then, the probe is transferred to the tumor free contralateral breast to include the mirror image location of the suspected cancer. The sensors giving the largest changes with respect to the mirror image position on the contralateral breast are related to the suspected cancer.

C. Feature Extraction

In this study, three features, namely, relative blood concentration, ΔBV, oxygen saturation, $\Delta Deoxy$, and the size of the tumor, S, are used.

The features, ΔBV, and $\Delta Deoxy$ are obtained using

$$\Delta OD = \varepsilon \Delta CL \tag{1}$$

where OD is the optical density, ε is the extinction coefficient, C is blood concentration, L is the mean pathlength of photons, and Δ denotes relative change. Here, $\varepsilon \approx 1$ cm^{-1}, and $L = 4$ cm for a pathlength factor of 5.

Following (1), the relative blood concentration, ΔBV, and the oxygen saturation, $\Delta Deoxy$, can be approximated at two different wavelengths by

$$\Delta BV \propto 0.3\Delta OD_{730} + \Delta OD_{850} \tag{2}$$

$$\Delta Deoxy \propto 1.3\Delta OD_{730} + \Delta OD_{850} \tag{3}$$

where ΔOD_{730}, and ΔOD_{850} denote the relative changes in optical density at 730 nm and 850 nm, respectively.

ΔBV and $\Delta Deoxy$ can also be approximated by

$$\Delta BV \propto \Delta[Hb] + \Delta[HbO_2] \tag{4}$$

$$\Delta Deoxy \propto \Delta[HbO_2] - \Delta[Hb] \tag{5}$$

where $\Delta[Hb]$, and $\Delta[HbO_2]$ denote the relative change in deoxyhemoglobin (Hb) and oxyhemoglobin (Hb0_2).

The concentrations of Hb, and HbO_2 in (4) and (5) are calculated by the Beer-Lambert Law given by

$$\Delta OD = log\frac{I_0}{I} \tag{6}$$

where I is light intensity after absorption and scattering, and I_0 is the baseline light intensity obtained from the contralateral breast, using known extinction coefficients of Hb, HbO_2 and differential pathlength factors [10].

Here, it is important to note that, ΔBV, and $\Delta Deoxy$ values are based on a lipid blood oxygen model. Thus the increments of BV and $Deoxy$ are relative to the contralateral breast:

$$\Delta BV = \Delta BV_{tumor} - \Delta BV_{contra} \tag{7}$$

$$\Delta Deoxy = \Delta Deoxy_{tumor} - \Delta Deoxy_{contra} \tag{8}$$

where ΔBV_{tumor}, ΔBV_{contra} are relative blood volume in the tumor breast and the mirror image position of the contralateral breast, respectively, and $\Delta Deoxy_{tumor}$, $\Delta Deoxy_{contra}$ are relative oxygen saturation in the tumor breast and the mirror image position of the contralateral breast, respectively.

D. Feature Analysis and Tumor Classification

In this subsection, we present the set of tumor classification features, and the malignancy differentiation criteria. F1 denotes ΔBV, F2 denotes $\Delta Deoxy$, and F3 denotes, S, size of the tumor. We evaluate the malignancy differentiation capability of the individual features and various combinations of the these features using a set of classifiers, namely, k-nearest neighbor classifier (KNNC), Parzen density based classifier (PAR), automatic neural network classifier (NEURC), normal densities based linear classifier (LDC), nearest mean classifier (NMC), scaled nearest mean classifier (NMSC), normal densities based quadratic classifier (QDC), uncorrelated normal densities based quadratic classifier (UDC). The more details information on these classifiers can be found in [12].

We evaluated the malignancy differentiation capability of the following individual and combined features:
F1: ΔBV
F2 : $\Delta Deoxy$
F3 : Tumor Size (S)
F1-F2: ΔBV and $\Delta Deoxy$
F1-F2-F3: ΔBV, $\Delta Deoxy$, and S

III. Statistical Analysis of Clinical Data

The evaluation is based on receiver operating characteristics (ROC) methodology. The ROC curve is obtained by plotting the probability of false positive rate versus the probability of detection. The evaluation of classification method is done using area under the ROC curve (AUC). First, we evaluated the classification performance of all three features. Table I presents the AUC values for 8 different classifiers for all three features. The NMSC has the best performance in terms of classification with a AUC value of 0.9098 followed by the Parzen classifier with a AUC value of 0.9041.

TABLE I

AUC VALUES FOR DIFFERENT CLASSIFIERS FOR F1-F2-F3: ΔBV, $\Delta Deoxy$, S

Type	**NMSC**	PAR	LDC	UDC	NEURC	QDC	NMC	KNNC
AUC	**0.9098**	0.9041	0.9017	0.8984	0.8864	0.8843	0.8807	0.8752

TABLE II

AUC VALUES FOR DIFFERENT CLASSIFIERS FOR F1-F2: ΔBV, $\Delta Deoxy$

Type	**NMSC**	PAR	LDC	UDC	NEURC	QDC	NMC	KNNC
AUC	**0.9001**	0.8993	0.8930	0.8908	0.8992	0.8821	0.8782	0.8645

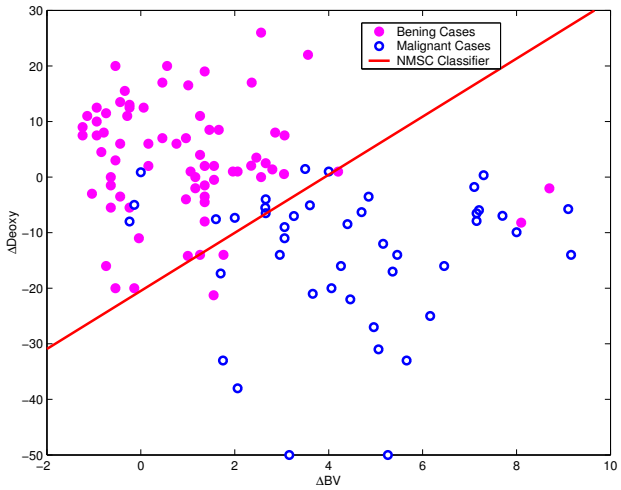

Fig. 2. Scaled Nearest Mean Classifier and F1-F2 2-D data clustering.

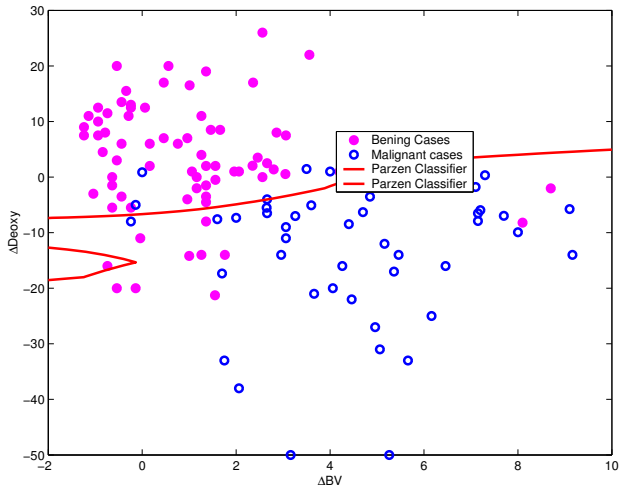

Fig. 3. Parzen and F1-F2 2-D data clustering.

Next, we evaluated the performance of the two features measured by NIR spectroscopy. Table II presents the AUC values for 8 different classifiers for features ΔBV and $\Delta Deoxy$. Again, the NMSC performed the best in terms of classification with a AUC value of 0.9001. Finally, we evaluated the individual classification performances of the three features. Table III presents the AUC values for 8 different classifiers for the feature ΔBV. The NMC has the best performance in terms of classification with a AUC value of 0.8832. Table IV presents the results 8 different classifiers for the feature $\Delta Deoxy$. The NMC has the best performance in terms of classification with a AUC value of 0.879. Table V presents the results 8 different classifiers for the feature S. The QDC has the best performance in terms of classification with a AUC value of 0.5612.

As it can be seen from Tables I, and II, the best performing feature set is the combination of the three features. We can also conclude from Table V that, the tumor size can not be used to differentiate healthy and diseased tissues with an AUC value of around 0.5. However, the combination set of optical indices, obtained using optical measurements, can differentiate breast tumors with a relatively high precision with a AUC value of 0.9. Similarly, optical indices, ΔBV and $\Delta Deoxy$, also performed well with AUC values of 0.883 and 0.879, respectively.

Figures 2, and 3 show the distribution of features ΔBV, and $\Delta Deoxy$ extracted from benign and malignant tumors. The thresholds were computed using scaled nearest mean classifier and Parzen classifiers. Figure 4 presents, the ROC curves for all three features, and the best two features, namely, $\Delta Deoxy$ and ΔBV. The observed area under the ROC curve for F1-F2-F3, and F1-F2 are 0.9098, and 0.9001, respectively. Figure 5 presents the ROC curves for individual features F1, and F2 using the nearest mean classifier. The observed area under the ROC curve for F1, and F2 are 0.8832 and 0.8790, respectively.

IV. CONCLUSION

In this work, we evaluated the characterization efficiency NIR optical spectroscopy using three features, relative blood concentration, oxygen saturation, and the size of the tumor. The characterization of malignant and benign tumors are evaluated using different classifiers. Our results suggest that the relative blood concentration, and oxygen saturation has potential to differentiate malignant and benign breast tumors with a relatively high accuracy. This set of features can potentially be incorporated into a diagnostic systems to aid physicians for breast cancer diagnosis. In the near future, we will incorporate additional features to the current feature set. We plan to analyze the new set of features using different

TABLE III

AUC VALUES FOR DIFFERENT CLASSIFIERS FOR F1: ΔBV

Type	NMSC	PAR	LDC	UDC	NEURC	QDC	**NMC**	KNNC
AUC	0.8817	0.8764	0.8807	0.8779	0.8513	0.8778	**0.8832**	0.8302

TABLE IV

AUC VALUES FOR DIFFERENT CLASSIFIERS FOR F2: $\Delta Deoxy$

Type	NMSC	PAR	LDC	UDC	NEURC	QDC	**NMC**	KNNC
AUC	0.8787	0.8764	0.8776	0.8711	0.8491	0.8613	**0.8790**	0.8331

TABLE V

AUC VALUES FOR DIFFERENT CLASSIFIERS FOR F3: S

Type	NMSC	PAR	LDC	UDC	NEURC	**QDC**	NMC	KNNC
AUC	0.5123	0.5292	0.4782	0.5429	0.5382	**0.5612**	0.5112	0.4827

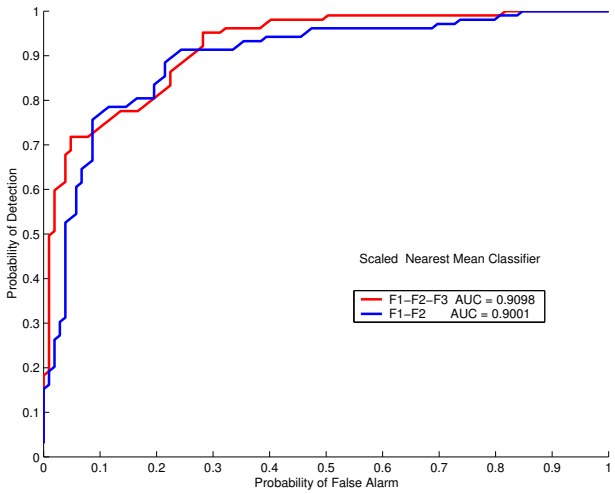

Fig. 4. ROC curves for F1-F2-F3 and F1-F2 using NMSC Classifier.

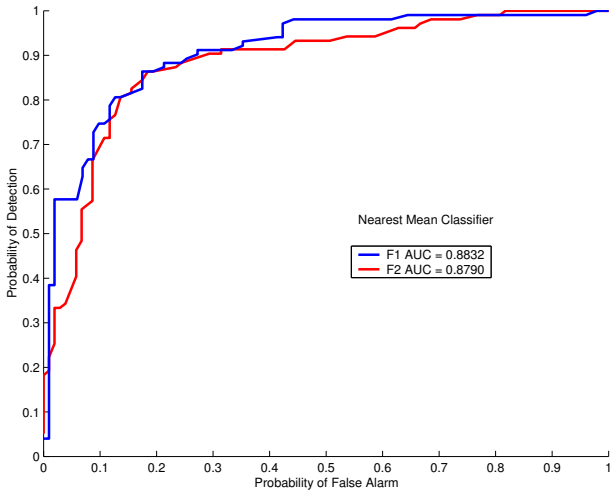

Fig. 5. ROC curves for F1and F2 using NMC Classifier.

sampling techniques, i.e. hold-out, leave-one-out, resubstitution techniques, and further investigate the characterization efficiency optical features. We also plan to compare the ROC performance of the optical features, F1 and F2, with that of F3, using a hypothesis testing method based on the AUC statistics.

REFERENCES

[1] American cancer society, statistics for 2006: http://www.cancer.org/

[2] Report of the Joint Working Group on Quantitative In Vivo Functional Imaging in Oncology, Sponsored by the *U.S. Public Health Services Office on Womens Health* and *National Cancer Institute*, 1999.

[3] B. W. Pogue, S. Jiang, H. Dehghani, C. Kogel, S. Soho, S. Srinivasan, X. Song, T. D. Tosteson, S. P. Poplack, K. D. Paulsen, "Characterization of hemoglobin, water, and NIR scattering in breast tissue: analysis of intersubject variability and menstrual cycle changes," *Journal of Biomedical Optics*, Vol. 9(3), pp. 541552, 2004.

[4] D. Grosenick, H. Wabnitz, K T. Moesta, J. Mucke, M. Mller, C. Stroszczynski, J. Stel, B. Wassermann, P. M. Schlag, and H. Rinneberg, "Concentration and oxygen saturation of haemoglobin of 50 breast tumours determined by time-domain optical mammography," *Phys. Med. Biol.* Vol. 49 No. 7, pp. 1165-1181, 2004.

[5] M. Khayat, Z. Ichalalene, N. Mincu, F. Leblond, O. Guilman, and S. Djeziri, "Optical tomography as adjunct to x-ray mammography: methods and results," *Proc. of SPIE*, Vol. 6431 64310F-1, 2007.

[6] B. J. Tromberg, N. Shah, R. Lanning, A. Cerussi, J. Espinoza, T. Pham, L. Svaasand, and J. Butler, Non-invasive in vivo characterization of breast tumors using photon migration spectroscopy, Neoplasia Vol. 2 (12), pp. 2640, 2000.

[7] V. Ntziachristos, B. Chance, "Probing physiology and molecular function using optical imaging: applications to breast cancer," *Breast Cancer Res.*, Vol. 3, pp. 41-46, 2001.

[8] P. Vaupel, A. Mayer, S. Briest, and M. Hockel, "Oxygenation gain factor: a novel parameter characterizing the association between hemoglobin level and the oxygenation status of breast cancers," *Cancer Res.*, Vol. 63, pp. 76347637, 2003.

[9] B. Chance, S. Nioka, J. Zhang, E. F. Conant, E. Hwang, S. Briest, S. G. Orel, M. D. Schnall, B. J. Czerniecki, "Breast cancer detection based on incremental biochemical and physiological properties of breast cancers: a six-year, two-site study," *Academic Radiology*, Vol. 12, Issue 8, pp. 925-933, 2005.

[10] S. Fantini, D. Hueber, M. A. Franceschini, E. Gratton, W. Rosenfeld, P. G. Stubblefield, D. Maulik, M. R. Stankovic, "Non-invasive optical monitoring of the newborn piglet brain using continuous-wave and frequency-domain spectroscopy," *Phys. Med. Biol.*, Vol. 44, pp. 1543-1563, 1999.

[11] K. Fukunaga, *Introduction to Statistical Pattern Recognition*, New York:Academic Press, 1990.

[12] R. O. Duda, P. E. Hart, D. G. Stork, *Pattern Classification*, New York: Wiley-Interscience, 2000.